Spinal Muscular Atrophy with Pontocerebellar Hypoplasia Is Caused by a Mutation in the *VRK1* Gene

Paul Renbaum,[1] Efrat Kellerman,[1,2] Ranit Jaron,[1,3] Dan Geiger,[4] Reeval Segel,[1,2,3] Ming Lee,[5] Mary Claire King,[5] and Ephrat Levy-Lahad[1,2,*]

The spinal muscular atrophies (SMAs) are a genetically and clinically heterogeneous group of disorders characterized by degeneration and loss of anterior horn cells in the spinal cord, leading to muscle weakness and atrophy. Spinal muscular atrophy with pontocerebellar hypoplasia (SMA-PCH, also known as pontocerebellar hypoplasia type 1 [PCH1]) is one of the rare infantile SMA variants that include additional clinical manifestations, and its genetic basis is unknown. We used a homozygosity mapping and positional cloning approach in a consanguineous family of Ashkenazi Jewish origin and identified a nonsense mutation in the vaccinia-related kinase 1 gene (*VRK1*) as a cause of SMA-PCH. *VRK1*, one of three members of the mammalian VRK family, is a serine/threonine kinase that phosphorylates p53 and CREB and is essential for nuclear envelope formation. Its identification as a gene involved in SMA-PCH implies new roles for the VRK proteins in neuronal development and maintenance and suggests the VRK genes as candidates for related phenotypes.

The spinal muscular atrophies (SMAs) are a genetically and clinically heterogeneous group of disorders characterized by degeneration and loss of anterior horn cells in the spinal cord, leading to muscle weakness and atrophy.[1] Proximal SMA (types I–IV [MIM 253300, 253550, 253400, 271150]) accounts for 80%–90% of all SMA cases and is primarily caused by recessive mutations in *SMN1* (MIM 600354), with homozygous absence of exon 7 in > 95% of cases.[2] Non-*SMN1* SMAs include nonproximal SMA (MIM 181405, 182960, 271220, 600794, 605726, 607088, 611067), bulbar palsy (MIM 211500, 211530, 601104), spinobulbar muscular atrophy (SBMA [MIM 313200]), and infantile SMA variants also known as "SMA plus."[1] These variants are characterized by SMA with additional or atypical features. They include SMA with respiratory distress (SMARD [MIM 604320]), which can be caused by recessive mutations in *IGHMBP2* (MIM 600502); infantile lethal X-linked SMA with arthrogryposis and congenital fractures (SMAX2 [MIM 301830]), caused by mutations in *UBE1* (MIM 314370); SMA1 with arthrogryposis and bone fractures (MIM 271225), which is yet to be mapped; and SMA with pontocerebellar hypoplasia (SMA-PCH [MIM 607596]), also known as PCH type 1. SMA-PCH is also associated with polyhydramnios, congenital contractures (secondary to reduced fetal movement), and respiratory insufficiency, leading to early death (mostly before 1 yr) in the original cases described.[3] However, in recent years, a broader clinical spectrum has emerged, with later onset of hypotonia, varying degrees of cerebellar or pontine hypoplasia and atrophy, peripheral nerve involvement, and longer survival.[4]

SMA-PCH is regarded as a subtype of both SMA and PCH and is also known as PCH1 (MIM 607596). All PCH syndromes include a small cerebellum and brainstem, and progressive microcephaly is common. The six currently described PCH subtypes are distinguished by additional features (OMIM; see Web Resources). SMA is found only in PCH1. PCH2, which is genetically heterogeneous (MIM 277470, 612389, 612390), is characterized by progressive cerebral atrophy, extrapyramidal dyskinesia and chorea, seizures, lack of motor and mental development, and normal spinal cord findings. PCH3 (MIM 608027), mapped to choromosome 7 in a single family, is characterized by optic atrophy, seizures, truncal hypotonia, specific facial features, and lack of extrapyramidal symptoms. PCH4 (MIM 225753) is a severe form with infantile encephalopathy, olivopontine atrophy, and early lethality. In PCH5 (MIM 610204), described in a single family, there is fetal onset of a seizure-like activity and severe olivopontocerebellar hypoplasia. PCH6 is a single-family, fatal, infantile form with mitochondrial respiratory chain defects and lack of motor or mental development. Interestingly, all genes so far identified as mutated in PCH are involved in tRNA processing: PCH2A and PCH4 are caused by *TSEN54* (MIM 608755) mutations,[5] PCH2B (MIM 612389) is caused by *TSEN2* (MIM 608753) mutations,[5] and PCH2C (MIM 612390) is caused by *TSEN34* (MIM 608754) mutations.[5] These genes encode noncatalytic (TSEN54) and catalytic (TSEN2 and TSEN34) subunits of the tRNA splicing endonuclease. PCH6 is caused by mutations in mitochondrial arginyl-tRNA synthetase (*RARS2* [MIM 611524]).[6]

The genetic basis of SMA-PCH has not been determined. The *SMN1* locus has been excluded in SMA-PCH, and tRNA defects identified in other forms of PCH during the course of our study were excluded on the basis of genomic location.

We report a consanguineous family of Ashkenazi Jewish origin, including three children with SMA-PCH (Figure 1).

[1]Medical Genetics Institute, Shaare Zedek Medical Center, Jerusalem 91031, Israel; [2]Hebrew University Medical School, Jerusalem, 91120, Israel; [3]Department of Pediatrics, Shaare Zedek Medical Center, Jerusalem 91031, Israel; [4]Computer Science Department, Technion, Haifa, 32000, Israel; [5]Departments of Medicine (Medical Genetics) and Genome Sciences, University of Washington, Seattle, WA 98195, USA
*Correspondence: lahad@szmc.org.il
DOI 10.1016/j.ajhg.2009.07.006.

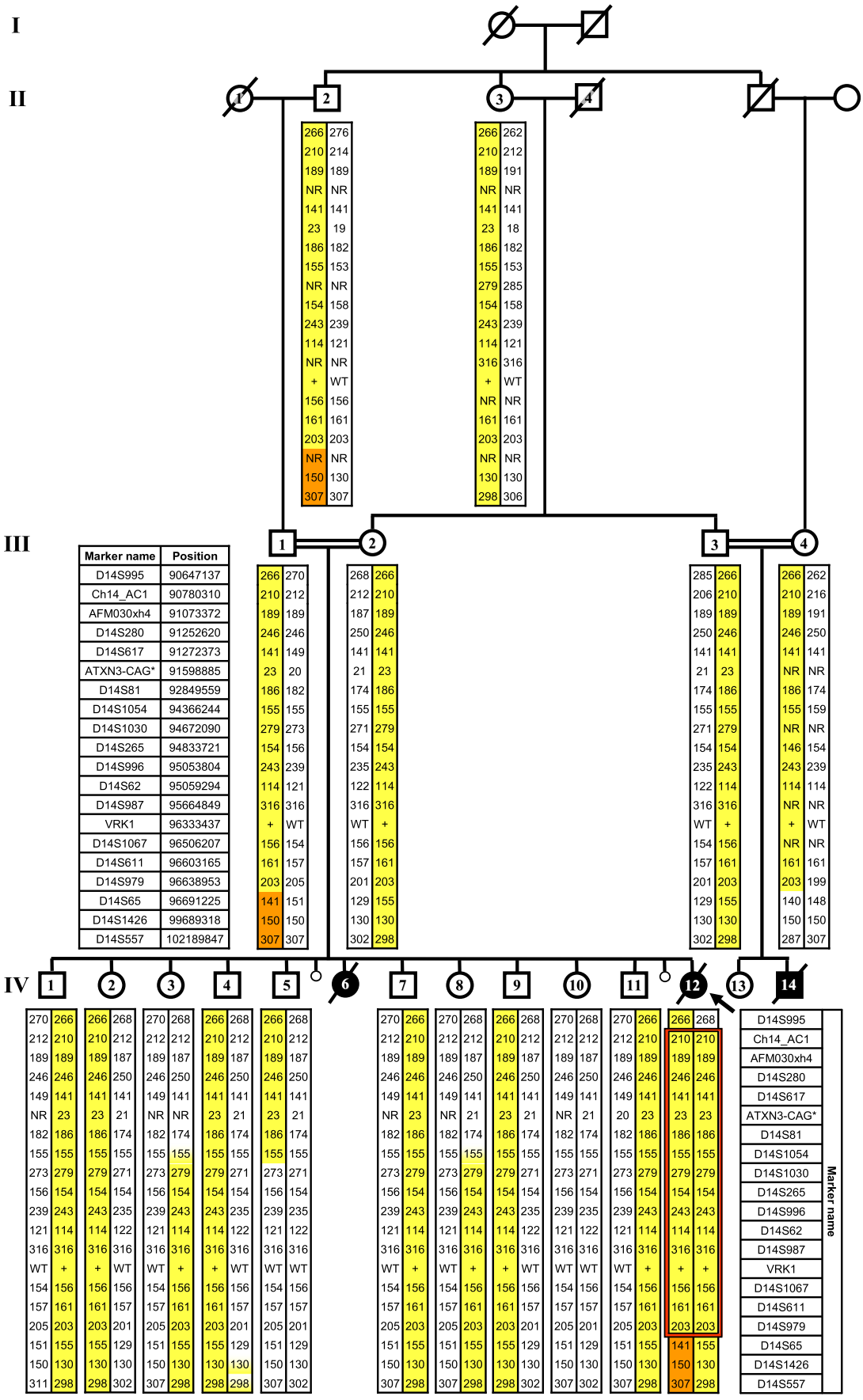

Marker name	Position
D14S995	90647137
Ch14_AC1	90780310
AFM030xh4	91073372
D14S280	91252620
D14S617	91272373
ATXN3-CAG*	91598885
D14S81	92849559
D14S1054	94366244
D14S1030	94672090
D14S265	94833721
D14S996	95053804
D14S62	95059294
D14S987	95664849
VRK1	96333437
D14S1067	96506207
D14S611	96603165
D14S979	96638953
D14S65	96691225
D14S1426	99689318
D14S557	102189847

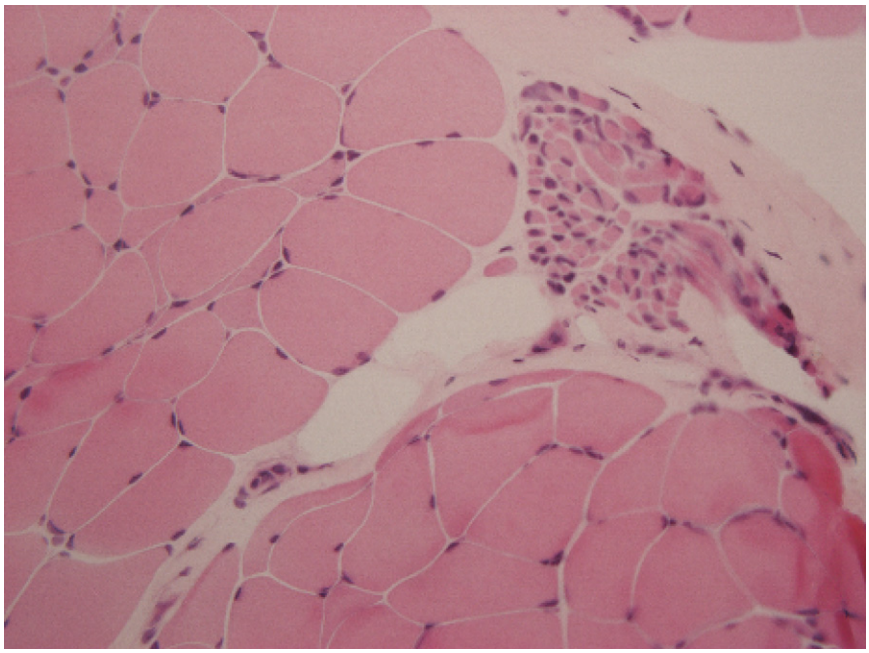

Figure 2. Muscle Biopsy of the Proband at Age 3 Yrs
Frozen hematoxylin-eosin-stained section shows bundles of larger-diameter fibers adjacent to bundles of very small fibers. Intermingled with the large fibers are a few angular fibers, singly and in small groups. There is no abundance of central nuclei, necrosis, regeneration, or other fiber structural changes. Collagen encircling atrophic fibers is observed.

The proband (IV-12) was the youngest daughter of first-cousin parents. Pregnancy was remarkable only for microcephaly noted on ultrasound at 7 mo gestation. At birth, weight was 2750 g, head circumference (HC) was 28.5cm (−6 SD), and poor sucking was noted. Brain CT was unremarkable except for microcephaly, and there was no evidence of craniosynostosis on skull X-rays. TORCH serology was negative. HC at 19 mo of age was 38 cm (−7.9 SD). Developmental delay became evident during the first two years (sitting at age 1 yr, assisted walking at 2 yrs), and the proband developed upper limb ataxia, brisk deep tendon reflexes (DTRs), and bilateral equinovarus. Results of electromyography (EMG), nerve conduction velocity (NCV), and somatosensory evoked potential (SEP) studies performed at age 2 yrs were consistent with motor and sensory neuropathy due to chronic denervation, more evident peripherally. Specifically, NCVs were normal, SEP showed diminished sensory nerve action potential (SNAP) in the right sural nerve, and EMG revealed fasciculations and fibrillations, consistent with motor neuron disease. At age 3 yrs, brain MRI showed a small cerebellar vermis and a large cisterna magna, compatible with cerebellar hypoplasia, and spine MRI was normal. (The MRI was performed in 1994 at a private facility, and images are unfortunately unavailable). Concurrently, a sural nerve biopsy was normal and muscle biopsy showed neurogenic atrophy typical of SMA (Figure 2). Cognitive ability was assessed as mild mental retardation. After corrective surgery, the proband began walking independently at age 3 yrs, though with ataxia. Additional studies at age 8 yrs included electron microscopy of a skin biopsy and isoelectric focusing of serum transferrin, which were both normal. Creatine phosphokinase (CPK) was not elevated (40 IU/l), and urinary organic acids were normal. Disease progression led to severe weakness, and the child became wheelchair-bound and incontinent, with sleep disturbance, increasing swallowing difficulties, severe ataxia, and progressive intercostal muscle weakness. A percutaneous gastrostomy was performed to allow feeding, but a few days after this procedure, the proband died at age 11.5 yrs. Testing for deletion of exon 7 in *SMN1* was negative.

The proband had a previously deceased older sister (IV-6) who was treated at another institution for the same condition. Review of her clinical records showed that after a normal pregnancy, birthweight was 3100 g and microcephaly was noted (HC 30.5 cm [−3 SD]). Investigations for microcephaly included skull X-rays, optic fundi examination, and TORCH serology, all of which were normal. She gained weight slowly but was otherwise healthy. Delayed motor milestones were apparent in the first year (rolling over at 8 mo, sitting at 15 mo, standing at 18 mo). Early language and social skills developed appropriately. Investigations at 6 mo included repeated skull X-rays demonstrating closure of skull sutures. EEG showed abnormal generalized discharges. Auditory brainstem response (ABR), visual evoked potential (VEP), and electroretinography (ERG) were normal. Brain CT scan showed mild bilateral enlargement of the posterior horns of the lateral ventricles, a large cisterna magna, and minimal cortical atrophy. Neurological examination at 2 yrs showed tongue fasciculations, hypotonia with brisk DTRs, and ataxia. Concurrently, she was noted to have bilateral equinovarus deformities, which necessitated splinting. At age 3 yrs, she was enrolled in a special education program. General functioning was severely impaired by ataxia, but language comprehension and social skills were relatively spared. At age 5 yrs, she could crawl on her knees independently

Figure 1. Linkage and Homozygosity Mapping of Markers on 14q32 to SMA-PCH in a Consanguineous Family
Affected individuals are shown in black. STR genotypes in the critical region are shown below each sampled individual, where numbers indicate amplicon size (bp). The disease-associated haplotype is shaded in yellow or yellow-orange. Only IV-12 is homozygous by descent for the region boxed in red.

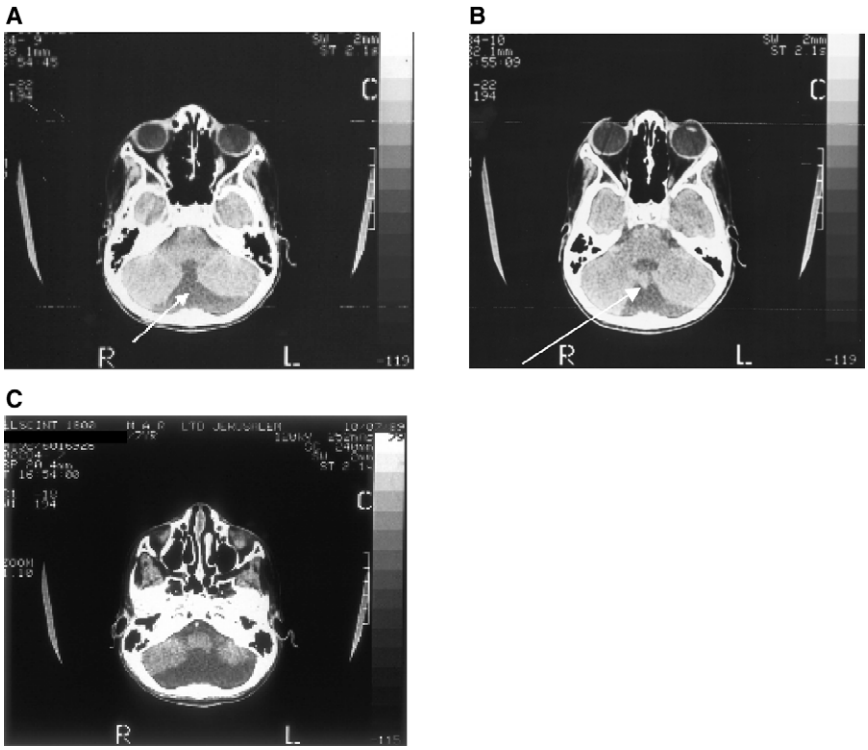

Figure 3. Brain CT Scan of the Proband's Sister at Age 7 Yrs, in 1989
(A) Cerebellar vermis hypoplasia, communicating fourth ventricle and cisterna magna (arrow).
(B) Cerebellar vermis hypoplasia (arrow).
(C) Large cisterna magna and cerebellar hemisphere hypoplasia.

and walk with the aid of a walker and braces. Examination revealed progressive microcephaly (HC 42.5cm [−6 SD]), distal muscle atrophy, brisk DTRs, no nystagmus, and obvious hand tremor and ataxia. EMG and NCV at this time showed demyelinating peripheral neuropathy. CSF protein (age 6 yrs) was 24 mg%. Brain CT scan at age 7 yrs showed cerebellar hypoplasia with suspected pontine hypoplasia (Figure 3). A CT of the cervical spine was normal. Additional laboratory tests showed normal female karyotype (46,XX), negative urinary oligosaccharides, and normal activity levels of the following lysosomal enzymes: Hexosaminidase A (Tay-Sachs disease [MIM 272800]), Galactocerebrosidase (Krabbe disease [MIM 245200]), Arylsulfatase A (metachromatic leukodystrophy [MIM 250100]), and beta-Galactosidase 1 (GM1 gangliosidosis [MIM 230500]). At age 8 yrs, incontinence developed, muscle strength decreased, and she became nonambulatory. Sleep disturbances appeared and progressed, with frequent awakenings. At age 9 yrs, a percutaneous gastrostomy was inserted because of increasing feeding and swallowing difficulties. A muscle biopsy performed at that time revealed neurogenic atrophy typical of SMA. Her disease progressed and she died at age 9.5 yrs. The family refused autopsy for both daughters. To summarize, both sisters presented with motor neuron disease consistent with SMA: clinically prominent progressive muscular weakness, EMG reflecting chronic denervation (fasciculations and fibrillations), and typical muscle pathology (neurogenic atrophy; see Figure 2). Both had progressive microcephaly of prenatal onset, mental deficiency, and significant ataxia, correlated with cerebellar hypoplasia on brain imaging (Figure 3). There were equivocal features of sensory neuropathy and evidence for upper motor neuron involvement. The disease was progressive from infancy but protracted, with death at 9.5 and 11.5 years. Notably, both girls had normal birth weights and did not have congenital arthrogryposis. The disease process was symmetric; there were no seizures, dykinesia, or chorea and no evidence of severe respiratory distress or diaphragmatic dysfunction. Both sisters were independently diagnosed with SMA-PCH, by two different clinical teams. Their cousin (IV-14), also the product of a consanguineous marriage within the extended family, was reported by his parents to have had a similar phenotype. He died at age 8 yrs, and his medical records are unavailable.

After approval by an institutional review board and the National Helsinki Committee for Genetic Studies, homozygosity mapping was performed on the proband (IV-12), who was the single affected individual for whom DNA was available, and on all other available relatives (Figure 1). DNA isolated from blood was typed with the use of the Affymetrix GeneChip 250K Nsp SNP array. SNP data were examined for informative genomic regions that were longer than 5 Mb and homozygous in the proband but not in any of her healthy siblings. Boundaries of homozygous segments in the proband were defined by the presence of two heterozygous SNPs in any moving 10-SNP window. A single 6.24 Mb region on chromosome 14 (including 576 SNPs from rs7146008 at 90,663,054 to rs17095290 at 96,905,397) was identified as homozygous by descent only in the affected proband. In addition, linkage analysis on genome-wide SNP data was performed with the use of Superlink Online,[7,8] assuming autosomal-recessive inheritance of SMA-PCH, high penetrance (99%), rare frequency of the disease allele in the general population (0.001), and no phenocopies. A multipoint LOD score of 3.3 was obtained for a 200 kb interval within the 6.24 Mb chromosome 14 homozygous region. No other region fulfilled homozygosity criteria or had significant LOD scores. Fine mapping of the homozygous region with the use of short tandem repeat (STR) markers defined a minimal 6.04 Mb interval between D14S995 (cen) and D14S65 (tel) (Figure 1), a region containing 71 known and predicted genes (UCSC Genome Browser).

An obvious candidate gene in this region was Ataxin-3 (*ATXN3*), because expansion of a coding CAG repeat in *ATXN3* causes spinocerebellar ataxia type 3 (SCA3 or Machado-Joseph disease [MJD, MIM 109150]).[9] MJD is an autosomal-dominant, adult-onset disease, whereas SMA-PCH is an autosomal-recessive disease of prenatal or infantile onset, but the cerebellum and spinocerebellar tracts are major targets of both diseases, so conceivably, a recessive *ATXN3* mutation could lead to SMA-PCH. We examined this possibility as follows (data not shown): (1) All *ATXN3* exons (including 5′ and 3′ UTRs) were sequenced in both parents and the affected proband in both directions. No previously unreported variants were identified. (2) *ATXN3* CAG repeats were genotyped in the entire family (ATXN3-CAG, Figure 1), and no expansion was identified. (3) For the purpose of ruling out a nonexonic mutation affecting *ATXN3* regulation, allele-specific *ATXN3* expression was analyzed in cDNA from lymphoblastoid cell lines of both parents. Both parents (obligate carriers) were heterozygous for a known SNP (rs12895357) in exon 10 and for the ATXN3 CAG repeat. Semiquantitative RT-PCR revealed comparable biallelic expression of *ATXN3* in both assays in each parent. (4) *ATXN3* splicing patterns were tested in both parents and in unrelated control individuals. No differences were observed in six different RT-PCR amplicons spanning the entire *ATXN3* transcript. Other genes in the minimal homozygous region were prioritized on the basis of cerebellar and spinal cord expression via the use of publicly available data on tissue-specific expression (Genecards) and RT-PCR on human cerebellar RNA (Ambion, TX, USA). In addition, we assessed known human phenotypes and murine models of genes in the candidate region. The proband's DNA was fully sequenced for 27 genes in the region, and no mutations were found (Table 1).

Table 1. The SMA-PCH Chromosome 14 Homozygous Region—Genes Sequenced and Found to be Wild-Type in the Affected Proband

No.	Gene Symbol	MIM No.	Gene Name
1	*ASB2*	605759	Ankyrin repeat and SOCS box-containing 2
2	*ATXN3*	607047	Ataxin 3
3	*BDKRB1*	600337	Bradykinin receptor B1
4	*BDKRB2*	113503	Bradykinin receptor B2
5	*CHGA*	118910	Chromogranin A
6	*CPSF2*	606028	Cleavage and polyadenylation specific factor 2
7	*DDX24*	606181	DEAD (Asp-Glu-Ala-Asp) box polypeptide 24
8	*DICER1*	606241	Dicer 1
9	*FBLN5*	604580	Fibulin 5
10	*GPR68*	601404	G protein-coupled receptor 68
11	*GSC*	138890	Goosecoid homeobox
12	IFI27L2	611319	Interferon, alpha-inducible protein 27-like 2
13	*ITPK1*	601838	Inositol 1,3,4-triphosphate 5/6 kinase
14	*MOAP1*	609485	Modulator of apoptosis 1
15	*NDUFB1*	603837	NADH dehydrogenase (ubiquinone) 1 beta
16	*NESPRIN3*	610861	Nesprin 3
17	*OTUB2*	608338	OTU domain, ubiquitin aldehyde binding 2
18	*PAPOLA*	605553	Poly(A) polymerase alpha
19	*PRIMA1*	-	Proline-rich membrane anchor 1
20	*SERPINA3*	107280	Serine proteinase inhibitor, clade A, member 3
21	*SERPINA4*	147935	Serine proteinase inhibitor, clade A, member 4
22	*SERPINA5*	601841	Serine proteinase inhibitor, clade A, member 5
23	*SERPINA6*	122500	Serine proteinase inhibitor, clade A, member 6
24	*SERPINA9*	-	Serine proteinase inhibitor, clade A, member 9.
25	*SLC24A4*	609840	Solute carrier family 24, member 4, isoform 3
26	*TCL1A*	186960	T cell leukemia/lymphoma 1A (TCL1A), transcript variant 2
27	*TRIP11*	604505	thyroid hormone receptor interactor 11

In the *VRK1* (vaccinia related kinase) gene (MIM 602168), the proband was found to have a homozygous C>T transition in nt 4 of *VRK1* exon 12 (NM_003384, 1072 C>T; chr14:96,412,123 on hg18, NCBI Build 36.1, displayed on the UCSC Genome Browser), creating a stop codon (R358X) (Figure 4A) within a highly conserved KKRKK nuclear localization signal (NLS) (Figures 4B and 4C). Semiquantitative comparison of the expression patterns of mutant and wild-type alleles in the heterozygous parents suggests that the mutant sequence is associated with significantly lower mRNA levels than the wild-type, perhaps as a result of nonsense-mediated decay (Figure 4D). Familial segregation of the mutation was as expected, revealing that the proband's aunt (III-3) and uncle (III-4) are indeed both carriers of *VRK1* R358X.

VRK1 exon 12 was sequenced in 449 normal Ashkenazi Jewish controls, and two *VRK1* R358X carriers were identified. The allele frequency is therefore 1/449 (95% CI: 1/625–1/263), confirming the rarity of the SMA-PCH mutation.

VRK1 was originally identified as a novel serine-threonine kinase in a screen for genes enriched in fetal versus adult liver and involved in cell cycle regulation.[10] The *VRK1* gene (NM_003384) comprises 13 exons encoding a 1720 nt transcript, including a 106 bp 5′ UTR and a 423 bp 3′ UTR. *VRK1* encodes a 396 aa protein (NP_003375), with an N-terminal serine/threonine kinase domain (aa 173–185), a C-terminal NLS (residues 356–360), an endosomal and lysosomal targeting sequence (aa 304–320), and a basic-acidic-basic (BAB) motif at the C terminus (Figure 4B). Through homology searches, the mammalian VRK family was found to include two additional members: VRK2, which associates with the

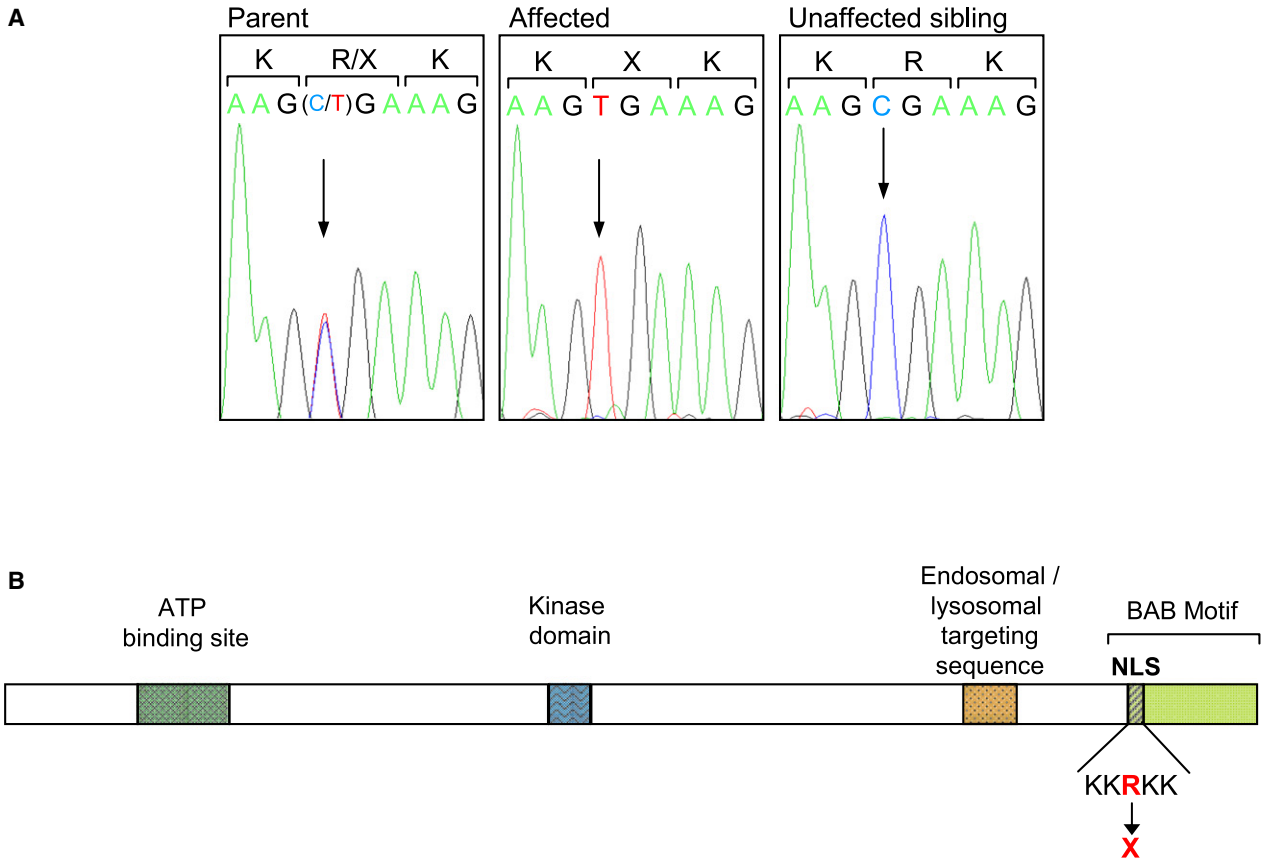
A
Parent
Affected
Unaffected sibling
K R/X K
K X K
K R K
A A G (C/T) G A A A G
A A G T G A A A G
A A G C G A A A G
B
ATP binding site
Kinase domain
Endosomal / lysosomal targeting sequence
BAB Motif
NLS
KKRKK
X
C
T
---> ATATGTAAGAAGCGAAAGAAAGAAATTGAA
UCSC Genes Based on Ref
VRK1
K R K K E I E
Vertebrate Multiz
Mammal Cons
Gaps
Human ATATGTAAG K R K K E I E
Rhesus ATCTGTAAG K R K K E M E
Mouse CTATGTAAG K R K K E A E
Dog GTATGTAAG K R K K G I E
Horse AAATGTAAG K R K K E I E
Armadillo ATGTGTAAG K R K K E T E
Opossum TTATATTAG K R K K E V E
Platypus TCGCAAAAG K R K K Q P E
D
ex12 C>T
ex8 rs2230532
Genomic DNA
cDNA
A A G (C/T) G A A
T G G (C/T) G T G

endoplasmic reticulum (ER) and the nuclear envelope (NE) and is enzymatically active, and VRK3, which is nuclear and enzymatically inactive as a result of key amino acid substitutions.[10,11] *C. elegans* and *Drosophila* have a single *VRK* ortholog, *CeVRK1* and *NHK1*, respectively.

VRK1 is ubiquitously expressed, including in fetal and adult brain and cerebellum ([10] and data not shown). At the subcellular level, it is mainly a nuclear protein, with a small fraction found in the cytoplasm and membrane compartments[11,12] (Human Protein Atlas). Dynamics of subcellular localization have not been studied in mammals, but in *Drosophila* and *C. elegans*, localization is cell-cycle-dependent: NHK-1 is cytoplasmic in the S phase, binds condensing chromatin in prophase, and is excluded from chromatin at the end of mitosis.[13] CeVRK-1 relocates to the nuclear rim just before mitosis and binds to chromatin from nuclear envelope breakdown until the end of mitosis.[14]

VRK1 function has been most extensively studied in the context of cellular proliferation and tumorigenesis (reviewed in [15]). VRK1 stabilizes p53 by phosphorylating its transactivation domain, thereby preventing its interaction with Mdm2. Normally, increased p53 proteolytically downregulates VRK1, but this autoregulatory loop is disrupted in a number of tumors, where increased VRK1 levels correlate with proliferation markers.[16] VRK1 also phosphorylates other transcription factors, including c-JUN, ATF-2, and CREB, and has recently been shown to be an early-response gene required for G1/S cell cycle progression,[17,18] at least in part through CREB-mediated regulation of cyclin D1 expression.[18] Identification of Myc as an activator of *VRK1* expression is further evidence of its significance for cellular proliferation.[18] In addition to these functions, VRK1 plays an important role in nuclear envelope and chromatin organization. VRK1 phosphorylates histone H3 during mitosis, and VRK inactivation in *C. elegans* and *Drosophila* results in chromatin hypercondensation.[19] In the nuclear envelope, VRK1 is essential for formation of nuclear membrane pore complexes, at least in part through its interaction with BAF (barrier to autointegration factor).[14] VRK1 phophorylates BAF during mitosis, thus releasing it from chromatin, to which it is bound during interphase.[14,20] BAF release is accompanied by release of nuclear lamina proteins, including emerin, a release critical for NE assembly. Lack of the single *VRK* gene in *Drosophila* is lethal.[21]

Our results suggest that in humans, *VRK1* deficiency causes a neurological phenotype that is both developmental and degenerative. Known VRK1 functions suggest interesting possibilities for its role in nervous system development and neuronal maintenance. Although *VRK1* has not been studied in this context, in mice, *VRK1* is expressed in the brain and spinal cord in all stages of development, including the adult (Allen Brain Atlas and data not shown). The VRK1/p53 autoregulatory loop may be relevant not only for malignancy but also for development and maintenance of the nervous system. p53 regulates cell division and death during nervous system development and in response to neuronal insult or injury during life (reviewed in [22]). Recessive mutations in *ATM*, which phosphorylates p53 in response to DNA damage, cause ataxia telangiectasia (MIM 208900), in which loss of cerebellar neurons and ataxia are prominent features. p53 interacts directly with SMN1, an association disrupted by SMN1 mutations associated with SMA,[23] although the relevance of this interaction to SMA pathogenesis is unclear.[24] Its role in the nuclear envelope may link VRK1 defects to the laminopathies, which have neuromuscular manifestations (reviewed in [25]). With respect to the essential role of VRK1 in BAF function, Baf null flies have small brains, missing imaginal discs, and defects in cell proliferation and differentiation in the thoracic ganglia and the brain hemispheres.[26] The role of VRK1 in CREB activation suggests that *VRK1* mutations may lead to impaired CREB signaling, which can result in both developmental and degenerative neurological disease. Coffin Lowry syndrome (MIM 303600) is caused by mutations in *RSK2*, another CREB kinase. Rubinstein Taybi syndrome (MIM 180849) can be caused by mutations in *CREBBP*, a CREB-binding protein. CREB depletion in the postnatal mouse brain leads to progressive neurodegeneration,[27] and interference with CREB-dependent transcription is a feature of polyglutamine stretches, common in spinocerebellar ataxias.[28] CREB also binds to the *SMN* promoter and increases *SMN* expression, so its deficiency could promote an SMA phenotype.[29]

As in any identification of a gene for a rare recessive disease in a single family, we cannot exclude the possibility of a deleterious mutation in one of the genes in the region that were not sequenced in the proband. However, the presence of a homozygous null mutation suggests that *VRK1* is very highly likely to be an SMA-PCH gene.

Figure 4. Homozygous *VRK1* Nonsense Mutation in SMA-PCH

(A) Genomic sequence of the VRK1 exon 12 region in informative family members. The proband is homozygous for a C>T transition that creates a TGA termination codon.

(B) Schematic representation of the VRK1 protein, including the ATP binding site, kinase domain, and nuclear leader sequence (NLS). Amino acid sequence of the NLS is indicated below, with the R358X mutation shown in red.

(C) Species conservation of amino acids in the R358X region.

(D) Allele-specific expression of VRK1 in R358X carriers. VRK1 exons 8 (ex8) and 12 (ex12) were sequenced in both genomic DNA and cDNA of a carrier of the R358X mutation. cDNA was extracted from an Epstein-Barr virus (EBV)-transformed B cell line. Exon 8 contains a known polymorphism (rs2230532) that also segregates in this family, and the exon 12 R358X mutation corresponds to 1072C>T in the cDNA (NM_003384). Top: genomic DNA sequences, showing equal biallelic content in both exon 8 and exon 12 sequences. Bottom: Unequal allelic expression in cDNA, where the wild-type allele predominates over the mutant (>70%).

Verification would require identification of additional patients with VRK1 mutations and additional studies addressing the mechanisms by which *VRK1* mutation leads to neuronal disease. Previous genes implicated in PCH without SMA are all involved in tRNA processing,[5,6] suggesting that *VRK1* may be specifically important for spinal motor neuron survival or that it may also play a role in tRNA processing. In either case, identification of a *VRK1* mutation as a cause of SMA-PCH points to new roles for this protein and suggests *VRK2* (chromosome 2p16) and *VRK3* (chromosome 19q13) as candidate genes for related phenotypes, including other pontocerebellar hypoplasias and other spinal muscular atrophies.

Acknowledgments

We thank Tom D. Bird of the Departments of Medicine and Neurology at the University of Washington, Seattle, WA, for reviewing the clinical information on the patients described in the study. Shirley Horn-Saban, Head of the Microarray Facility at the Weizmann Institute of Science, Rehovot, Israel, performed SNP genotyping. We thank Anna Tzemach for assistance with the genome-wide linkage analysis. We thank Hadassah Hartman for excellent secretarial assistance, and we thank all family members for their participation in this study. This research was supported by the Legacy Heritage Bio-Medical Program of the Israel Science Foundation (grant no. 1872/2008 to P.R. and E.L.L.), by the Israel Science Foundation (grant no. 1174/2007 to D.G.), and by a generous gift from Rabbi and Mrs. David Fuld to Shaare Zedek Medical Center.

Received: May 24, 2009
Revised: July 5, 2009
Accepted: July 13, 2009
Published online: July 30, 2009

Web Resources

The URLs for data presented herein are as follows:

Allen Brain Atlas, http://mouse.brain-map.org/
Genecards, http://www.genecards.org/
Human Protein Atlas, http://www.proteinatlas.org/
Online Mendelian Inheritance in Man (OMIM), http://www.ncbi.nlm.nih.gov/omim/
SuperLink, http://bioinfo.cs.technion.ac.il/superlink-online/
UCSC Genome Browser, http://genome.ucsc.edu

References

1. Zerres, K., and Rudnik-Schoneborn, S. (2006). Spinal muscular atrophies. In: Principles and Practice of Medical Genetics, 5th ed., D.L. Rimoin, J.M. Connor, R.E. Pyeritz, and B.R. Korf, eds. (New York, USA: Churchill Livingstone), pp. 3001–3023.
2. Wirth, B. (2000). An update of the mutation spectrum of the survival motor neuron gene (SMN1) in autosomal recessive spinal muscular atrophy (SMA). Hum. Mutat. *15*, 228–237.
3. Barth, P.G. (1993). Pontocerebellar hypoplasias: An overview of a group of inherited neurodegenerative disorders with fetal onset. Brain Dev. *15*, 411–422.
4. Rudnik-Schoneborn, S., Sztriha, L., Aithala, G.R., Houge, G., Laegreid, L.M., Seeger, J., Huppke, M., Wirth, B., and Zerres, K. (2003). Extended phenotype of pontocerebellar hypoplasia with infantile spinal muscular atrophy. Am. J. Med. Genet. A. *117*, 10–17.
5. Edvardson, S., Shaag, A., Kolesnikova, O., Gomori, J.M., Tarassov, I., Einbinder, T., Saada, E., and Elpeleg, O. (2007). Deleterious mutation in the mitochondrial arginyl-transfer RNA synthetase gene is associated with pontocerebellar hypoplasia. Am. J. Hum. Genet. *81*, 857–862.
6. Budde, B.S., Namavar, Y., Barth, P.G., Poll-The, B.T., Nurnberg, G., Becker, C., van Ruissen, F., Weterman, M.A.J., Fluiter, K., te Beek, E.T., et al. (2008). tRNA splicing endonuclease mutations cause pontocerebellar hypoplasia. Nat. Genet. *40*, 1113–1118.
7. Fishelson, M., and Geiger, D. (2002). Exact genetic linkage computations for general pedigrees. Bioinformatics *18* (*Suppl 1*), S189–S196.
8. Fishelson, M., Dovgolevsky, N., and Geige, D. (2005). Maximum likelihood haplotyping for general pedigrees. Hum. Hered. *59*, 41–60.
9. Kawaguchi, Y., Okamoto, T., Taniwaki, M., Aizawa, M., Inoue, M., Katayama, S., Kawakami, H., Nakamura, S., Nishimura, M., Akiguchi, I., et al. (1994). CAG expansions in a novel gene for Machado-Joseph disease at chromosome 14q32.1. Nat. Genet. *8*, 221–228.
10. Nezu, J., Oku, A., Jones, M.H., and Shimane, M. (1997). Identification of two novel human putative serine/threonine kinases, VRK1 and VRK2, with structural similarity to vaccinia virus B1R kinase. Genomics *45*, 327–331.
11. Nichols, R.J., and Traktman, P. (2004). Characterization of three paralogous members of the Mammalian vaccinia related kinase family. J. Biol. Chem. *279*, 7934–7946.
12. Valbuena, A., López-Sánchez, I., Vega, F.M., Sevilla, A., Sanz-García, M., Blanco, S., and Lazo, P.A. (2007). Identification of a dominant epitope in human vaccinia-related kinase 1 (VRK1) and detection of different intracellular subpopulations. Arch. Biochem. Biophys. *465*, 219–226.
13. Aihara, H., Nakagawa, T., Yasui, K., Ohta, T., Hirose, S., Dhomae, N., Takio, K., Kaneko, M., Takeshima, Y., Muramatsu, M., and Ito, T. (2004). Nucleosomal histone kinase-1 phosphorylates H2A Thr 119 during mitosis in the early Drosophila embryo. Genes Dev. *18*, 877–888.
14. Gorjánácz, M., Klerkx, E.P., Galy, V., Santarella, R., López-Iglesias, C., Askjaer, P., and Mattaj, I.W. (2007). Caenorhabditis elegans BAF-1 and its kinase VRK-1 participate directly in post-mitotic nuclear envelope assembly. EMBO J. *26*, 132–143.
15. Klerkx, E.P., Lazo, P.A., and Askjaer, P. (2009). Emerging biological functions of the vaccinia-related kinase (VRK) family. Histol. Histopathol. *24*, 749–759.
16. Santos, C.R., Rodríguez-Pinilla, M., Vega, F.M., Rodríguez-Peralto, J.L., Blanco, S., Sevilla, A., Valbuena, A., Hernández, T., van Wijnen, A.J., Li, F., et al. (2006). VRK1 signaling pathway in the context of the proliferation phenotype in head and neck squamous cell carcinoma. Mol. Cancer Res. *4*, 177–185.
17. Valbuena, A., López-Sánchez, I., and Lazo, P.A. (2008). Human VRK1 is an early response gene and its loss causes a block in cell cycle progression. PLoS ONE. *3*, e1642.
18. Kang, T.H., Park, D.Y., Kim, W., and Kim, K.T. (2008). VRK1 phosphorylates CREB and mediates CCND1 expression. J. Cell Sci. *121*, 3035–3041.
19. Kang, T.H., Park, D.Y., Choi, Y.H., Kim, K.J., Yoon, H.S., and Kim, K.T. (2007). Mitotic histone H3 phosphorylation by

vaccinia-related kinase 1 in mammalian cells. Mol. Cell. Biol. *27*, 8533–8546.
20. Nichols, R.J., Wiebe, M.S., and Traktman, P. (2006). The vaccinia-related kinases phosphorylate the N′ terminus of BAF, regulating its interaction with DNA and its retention in the nucleus. Mol. Biol. Cell *17*, 2451–2464.
21. Cullen, C.F., Brittle, A.L., Ito, T., and Ohkura, H. (2005). The conserved kinase NHK-1 is essential for mitotic progression and unifying acentrosomal meiotic spindles in Drosophila melanogaster. J. Cell Biol. *171*, 593–602.
22. Jacobs, W.B., Kaplan, D.R., and Miller, F.D. (2006). The p53 family in nervous system development and disease. J. Neurochem. *97*, 1571–1584.
23. Young, P.J., Day, P.M., Zhou, J., Androphy, E.J., Morris, G.E., and Lorson, C.L. (2002). A direct interaction between the survival motor neuron protein and p53 and its relationship to spinal muscular atrophy. J. Biol. Chem. *277*, 2852–2859.
24. Tsai, M.S., Chiu, Y.T., Wang, S.H., Hsieh-Li, H.M., and Li, H. (2006). Abolishing Trp53-dependent apoptosis does not benefit spinal muscular atrophy model mice. Eur. J. Hum. Genet. *14*, 372–375.
25. Capell, B.C., and Collins, F.S. (2006). Human laminopathies: nuclei gone genetically awry. Nat. Rev. Genet. *7*, 940–952.
26. Furukawa, K., Sugiyama, S., Osouda, S., Goto, H., Inagaki, M., Horigome, T., Omata, S., McConnell, M., Fisher, P.A., and Nishida, Y. (2003). Barrier-to-autointegration factor plays crucial roles in cell cycle progression and nuclear organization in Drosophila. J. Cell Sci. *116*, 3811–3823.
27. Mantamadiotis, T., Lemberger, T., Bleckmann, S.C., Kern, H., Kretz, O., Martin Villalba, A., Tronche, F., Kellendonk, C., Gau, D., Kapfhammer, J., et al. (2002). Disruption of CREB function in brain leads to neurodegeneration. Nat. Genet. *31*, 47–54.
28. Shimohata, T., Nakajima, T., Yamada, M., Uchida, C., Onodera, O., Naruse, S., Kimura, T., Koide, R., Nozaki, K., Sano, Y., et al. (2000). Expanded polyglutamine stretches interact with TAFII130, interfering with CREB-dependent transcription. Nat. Genet. *26*, 29–36.
29. Majumder, S., Varadharaj, S., Ghoshal, K., Monani, U., Burghes, A.H., and Jacob, S.T. (2004). Identification of a novel cyclic AMP-response element (CRE-II) and the role of CREB-1 in the cAMP-induced expression of the survival motor neuron (SMN) gene. J. Biol. Chem. *279*, 14803–14811.